Interface deformation and the parameters relevant to bubble detachment when gas is injected into polymer melt flow field

YE-BIN CAI
College of Mechanical Engineering, South China University of Technology, Guangzhou 510641, People's Republic of China; College of Electromechanical Engineering, Maoming University, Maoming 525000, People's Republic of China

MING-CHENG GUO
College of Mechanical Engineering, South China University of Technology, Guangzhou 510641, People's Republic of China

ZAI-LIANG CHEN
College of Electromechanical Engineering, Soochow University, Suzhou 250012, People's Republic of China

YU-CHENG PENG*, CUN-XI XIE
College of Mechanical Engineering, South China University of Technology, Guangzhou 510641, People's Republic of China
E-mail: pskcgong@sohu.com

In recent years, much research work has been focused on the blending of different polymers in order to acquire materials with more advantageous characteristics, therefore, the dispersion or deformation of the dispersed droplet phase suspended in another polymer melt has been the subject of many investigators [1–3]. Relative to this field of investigation, the deformation process of a single gas bubble has been studied under different flow fields yet little has been reported. However, the study of bubble deformation and breakup process under flow field is of great importance in many fields of investigation, such as foam processing [4, 5] and the devolatilization process [6–8]. For instance, during foam extrusion using physical blowing agent, the inert gas will first be injected into polymer melt, and for the special process of microcellular foaming, the uniform homogeneous polymer melt containing the dissolved foaming gas should be obtained in front of the nucleating unit. Then the transformation of injected gas bubble to the dissolved gas will deal with the bubble deformation and breakup process, and the extent of bubble dispersion and distribution in polymer melt is of critical importance to this transformation. The smaller the bubbles, the higher the dissolving rate.

Recently, Favelukis [9] made an experiment to show the deformation of a single gas bubble under the simple shear flow field of polymer solution. The result was similar to that of a single droplet and a deformed ellipsoidal shape was presented. We also have done some elementary experiments to show the bubble deformation process when gas was injected into static polymer melt and found that the melt elasticity arising from bubble growth will cause the bubble to deform towards the opposite direction of its dilatation [10, 11].

In this paper, gas will be injected into a polymer melt flow field through a nozzle and the bubble deformation process will be investigated. By changing the gas injection pressure, bubbles with different volume, surface area, as well as different detaching times will be obtained. When the bubbles move towards the die exit, the bubble interface then will be affected by the flow field, and thus its deformation process can be characterized. In addition, the parameters relevant to the bubble detachment, such as the detachment time ranging from the bubble emergence to its detachment, the magnitude of the bubble volume or its maximum diameter were investigated by changing all related experimental conditions.

The experimental setup consists of a visible die and a gas injection system. For the convenience of observation, the front and back sides of the channel are both equipped with quartz glasses to monitor and record the bubble formation process. A rectangular flow channel with uniform cross section, which is followed by a convergence channel is selected, as shown in Fig. 1. The width and height of the rectangular flow channel are 27 and 20 mm, respectively.

The gas injection system consists of a gas cylinder, a pressure release valve, a rotameter, a needle valve, manometers and a gas injection nozzle; the inner diameter of the nozzle is 2 mm. The gas injection position is located at about three-tenths the height of the channel from the upper edge.

The polymer melt in this study is polypropylene (CJS-700G, Sinopec Corp.) for its transparency; carbon dioxide (CO_2) (Guangzhou Gas Plant, Commercial grade) is selected as the injected gas. Properties of the two materials relevant to the interfacial deformation are summarized in Table I.

By regulating the opening of the pressure release valve and the needle valve, different gas injection pressures can be obtained, which is shown through a

*Author to whom all correspondence should be addressed.

0022–2461

TABLE I Material properties

Name	Density (kg/m^3)	Zero-shear viscosity (Pa·s)	Interfacial tension (dynes/cm)	Melt index (g/10 min)
CO_2	1.143 (200 °C, 1 atm)	2.28×10^{-6} (200°C, 1 atm)		
Polypropylene	910	5.7×10^3 (200 °C)	19.3 (200 °C)	9.6

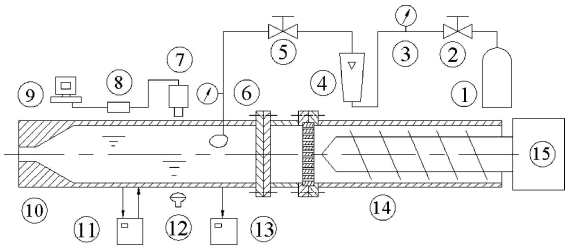

Figure 1 Experimental setup. 1. gas cylinder, 2. pressure release valve, 3. manometer, 4. rotameter, 5. needle valve, 6. manometer, 7. video camera, 8. digitizer, 9. personal computer, 10. die, 11. Const. temp. regulator, 12. Lamp, 13. pressure transducer, 14. extruder, 15. power system.

manometer mounted near the nozzle. Diameter of the screw is 20 mm and L/D is 25. All the experimental runs are made at isothermal conditions and a constant temperature regulator, which is set at 200 °C, controls the die temperature. When steady continuous bubble formation is found, the video system (video camera Vk-C220E, Hitachi Co., Ltd.) then begins to record, and the video signal is transmitted to a digital video processor. A personal computer is used to acquire images and to perform image analysis. In addition, there is a light source to produce silhouette image of bubbles.

When gas is injected into polymer melt, the pressure-driven flow will carry and push the bubble to transport along the uniform rectangular duct. When the tail of the bubble is still connected with the nozzle, the continuous gas addition into the bubble will make its volume increase on the one hand, and on the other hand, the flow field will also make the bubble interface deform, and thus will make the interface show different deformation process. In this investigation, four groups of experiments were made by varying the gas injection pressures (P_g) while maintaining the constant melt pressures (P_m) near the gas injection nozzle. The recorded bubble images for different time periods are shown in Fig. 2.

In the investigation of the parameters relevant to bubble detachment, three experimental conditions are changed individually, namely, the gas injection pressure P_g, the hydrostatic melt pressure P_m near the gas injection port, and the screw rotation speed n. P_g can be adjusted by regulating the opening of the pressure release valve and the needle valve; P_m can be changed by varying the screw rotation speed and by regulating the opening the convergence channel. The recorded bubble images at different time periods for the four groups of experiments are shown in Fig. 3.

Seen from Fig. 2, we can see that the Deformation of bubbles all experience three stages whatever the experimental conditions. The first stage is the emergence of bubble from the gas injection nozzle. Because of its small dimensions, the effect of flow field on bubble deformation is negligible and the nearly spherical or ellipsoidal shape is maintained. With its dilatation, the influence of flow field notably increases, with the bubble interface showing an approximately cone shape. When the bubble detaches from the nozzle, its deformation will be solely affected by the flow field. The shear stress of flow field will reduce the larger diameter of the bubble end, and transform it into a cylindrical shaped bubble. Moreover, the original one trailing end shape will eventually transform to a double-tip fishtail shape due to the pressure-driven flow.

In the first stage, owing to the small dimension of the bubble, the capillary number is also small; therefore, the radial dilatation is predominant and a spherical or ellipsoidal shape is initially assumed. With the volume increase of the bubble, the effect of flow field on the interface deformation cannot be neglected. From

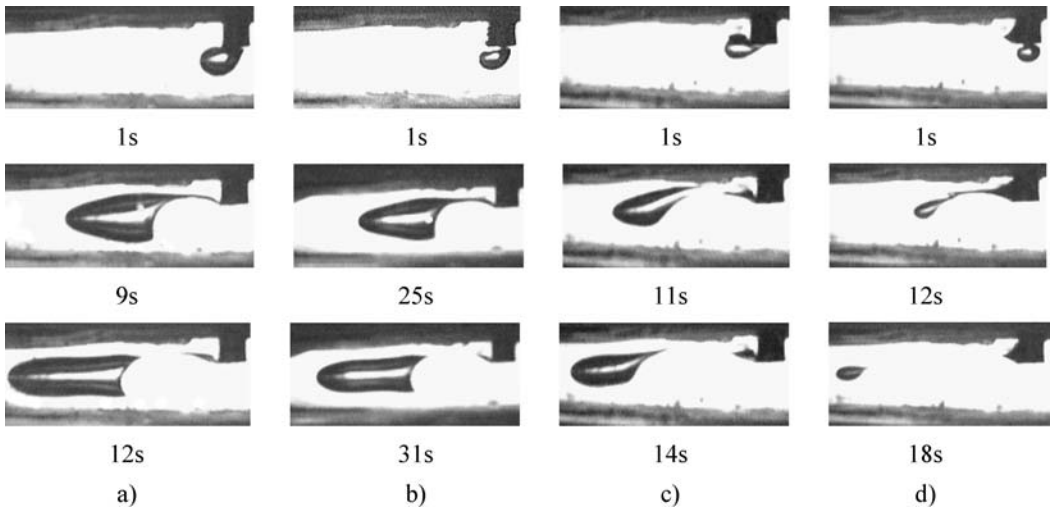

Figure 2 Recorded bubble images for different time periods under different experimental conditions, (a) $P_g = 0.25$ Mpa, $P_m = 0.15$ Mpa; (b) $P_g = 0.2$ Mpa, $P_m = 0.15$ Mpa; (c) $P_g = 0.18$ Mpa, $P_m = 0.15$ Mpa; (d) $P_g = 0.17$ Mpa, $P_m = 0.15$ Mpa.

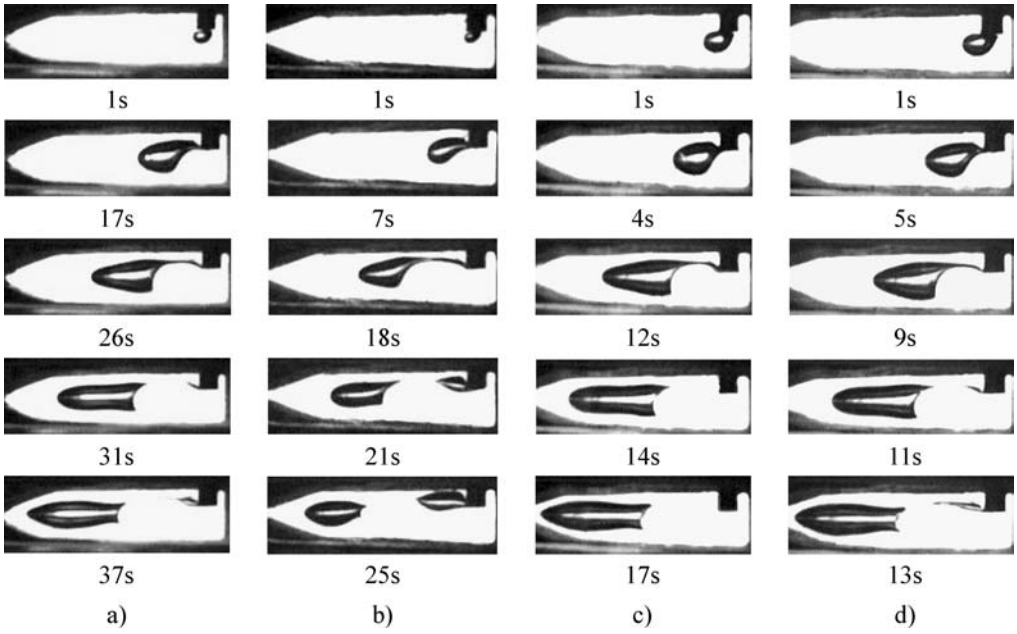

Figure 3 Recorded bubble images at different time periods under different experimental conditions, a) $P_g = 0.18$ Mpa, $P_m = 0.10$ Mpa, $n = 20$ rpm; (b) $P_g = 0.23$ Mpa, $P_m = 0.21$ Mpa, $n = 30$ rpm; (c) $P_g = 0.21$ Mpa, $P_m = 0.12$ Mpa, $n = 40$ rpm; (d) $P_g = 0.25$ Mpa, $P_m = 0.15$ Mpa, $n = 50$ rpm.

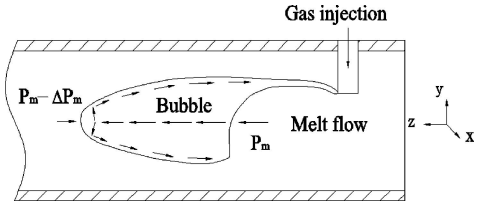

Figure 4 Schematic of the bubble deformation process.

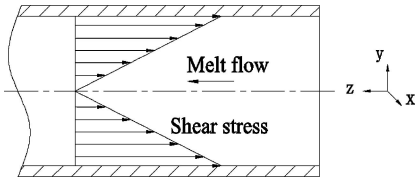

Figure 5 Schematic of the shear stress at the middle of the flow channel along width direction.

literature [12], we know that the increase of bubble radius is dependent upon the pressure difference between the gas and melt phases, the surface tension, the interface deformation rate, and so on. Therefore, the higher melt pressure near the tail of the bubble then will delay its radial dilatation, whereas, the relatively lower pressure near the head of the bubble, together with the aid of the transferred melt pressure from the tail of the bubble, will promote its dilatation, as shown in Fig. 4. As a result, the interface of the bubble, both the tail and the head will extend along the melt flow direction.

As we know, for steady, fully developed flow, an approximate parabola velocity profile at the middle of the flow channel will be shown for the non-Newtonian fluid. When the bubble expands to some extents, the pressure-driven flow will be blocked by the bubble and then the interface of its end section certainly will show the similar parabola shape to the melt flow rate due to their interaction. Apart from the above analysis, the shear stress also plays a very important role for the interface deformation. Schematic of the shear stress at the middle of the flow channel along width direction is shown in Fig. 5.

We can see that the existence of shear stress will delay the interface dilatation and movement along the flow direction, the closer to the wall, the stronger this effect. Therefore, a cone-shaped head of the bubble is presented.

When bubble detaches from the nozzle, the bubble volume increase ceases and only the flow field will control the interface deformation. On the one hand, the melt pressure will push the bubble move towards the exit direction, on the other hand, the shear stress will gradually reduce the larger diameter of the bubble end and finally show a cylindrical shape.

Seen from the experimental results, we can see that the gas–melt interface deformation is analogous to the droplet interface deformation. Different bubble interface shapes, such as the ellipsoidal shape under simple shear flow or the fishtail trailing end under pressure-driven flow both can be shown.

By changing the gas injection pressure, bubbles with different volumes can be obtained. For bubbles whose volume is comparative to the height of the flow channel, the above interface deformation analysis is suitable. While for small bubbles, as shown in Figs 2c and d, the situations will be a little different. Because of the decreased bubble volume, the gas fractional coverage along height of the channel is reduced, then under the pressure-driven flow, more fluid will flow towards the exit through the clearance of the bubble and the wall, and because of the upper injection position, the double-tip fishtail shape of the end will finally be replaced by a single tip shape, with the tail connecting to the gas injection nozzle, as shown in Fig. 6.

In addition, the experiments clearly show that when bubble moves towards the exit, it will migrate perpendicular to the streamline flow, and eventually it will migrate towards the center axis of the channel regardless

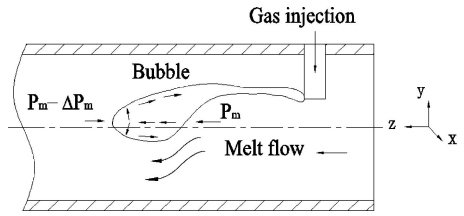

Figure 6 Schematic of the small bubble deformation.

of the volume of the bubble. This result is in accordance with C. D. Han's report [13].

Fig. 3 shows that under different experimental conditions, different bubbles as well as different deformation processes can be obtained. To compare the effects of experimental conditions on the bubble configurations, several typical parameters should be selected. Here, we select the bubble volume, bubble surface area and its maximum diameter to characterize its magnitude and configuration. These parameters are obtained by simulating the bubbles using a 3-D software. In addition, the bubble detachment time ranging from the emergence of bubbles to its detachment from the nozzle is also a very important parameter, which deals with the rate of bubble formation. Figs 7–9 show the variation of bubble volumes, surface areas and the maximum diameters during bubble formation with time under the four experimental conditions.

It can be seen that the variation of bubble volume and surface area with time for different experiments is very similar, and it is the pressure difference between the gas injection pressure and the melt pressure that decides the magnitude of the bubble, the larger the pressure difference, the bigger the bubble. But the variation of the maximum diameter is little different from the

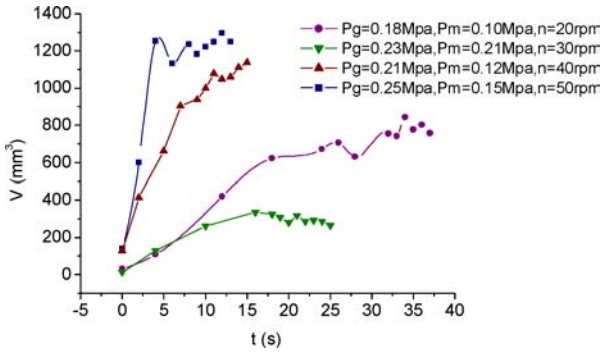

Figure 7 Variation of bubble volume with time.

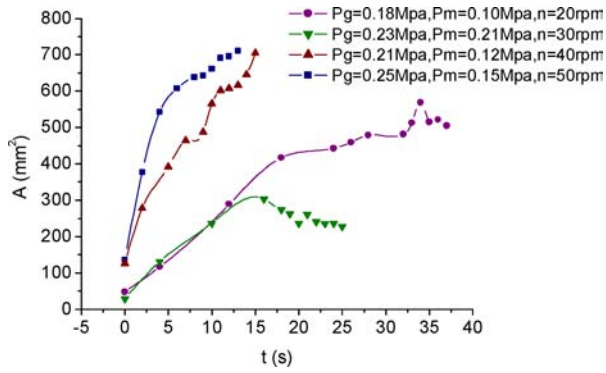

Figure 8 Variation of bubble surface area with time.

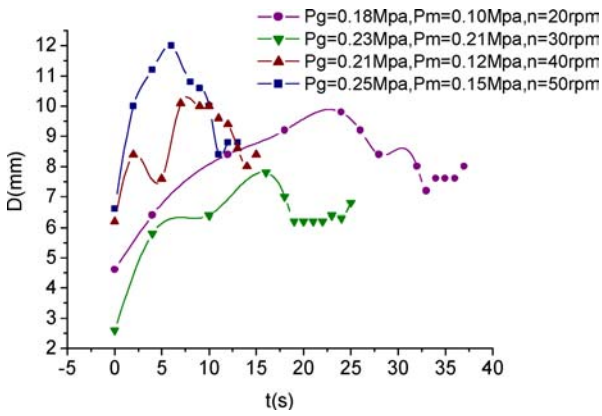

Figure 9 Variation of the maximum diameter of the bubble with time.

above two parameters. Seen from Fig. 9, we can see that for each experiment, the curve experiences a peak value, and then the maximum diameter decreases. As is analyzed, the shear stress is of critical importance on the reduction of the larger diameter of the bubble end when it detaches from the injection nozzle. Therefore, although we cannot yet distinguish the accurate time of bubble detachment from the nozzle using the video system, the time when the peak value occurs is suitably seen as the detachment time. It's evident that the bubble detachment time is mainly affected by the screw rotation speed, the higher speed will cause the bubble detach earlier. Since the higher screw speed means the higher melt flow rate, therefore, we think that it's the melt flow rate that is critical for the bubble detachment time.

Unlike the variation of the maximum diameter, the bubble volume and the surface area don't always experience peak value. For the experiments with high pressure difference, the bubble volume and surface area continue to increase even if the bubbles have detached from the nozzle, while for the low pressure difference, the situation is the same as that of the diameter, the bubble volume and the surface area both decrease after detaching from the nozzle. It's evident that the pressure difference is the major reason for these phenomena. In addition, the relatively high screw speed for experiment (b) in Fig. 3 should also have influence on it, since the bubble has already begun to enter the convergence region upon its detaching.

From the point of view of practical engineering, the magnitude of the bubble and the detachment time are the two most important parameters since they are directly related to the follow-up re-distribution or dispersion processes. Therefore, the effects of experimental conditions on the two parameters should be investigated in more detail. Equations 1 and 2 are the multianalysis linear regressive equations for the maximum diameter and the bubble detachment time. Four groups of experimental conditions described in Fig. 3 are used in the calculation.

$$D = -1.778 - 0.005n + 31.945(P_g - P_m) + 28.611P_g \quad (1)$$

$$t = 4.667 - 1.017n + 83.333(P_g - P_m) + 183.334P_g \quad (2)$$

It shows that the screw rotation speed and the pressure difference as well as the gas injection pressure have similar effects upon the maximum diameter and the detachment time. The increase of screw rotation speed is favorable to achieve little bubbles and to obtain the short detachment times, while the increase of the pressure difference is just the opposite. Therefore, in order to acquire little bubbles in short time, the melt flow rate near the injection port should be increased as large as possible, and the pressure difference should be maintained little as long as the gas can be injected into the melt.

When gas is injected into a polymer melt flow field, continuous bubble formation can be acquired, and by varying the gas injection pressure, bubbles with different volumes can be obtained. Although the bubble volumes are different, their deformation all experience three distinct stages, namely, the approximate spherical or ellipsoidal shape at the first stage, the cone shape while it's dilating, and the cylindrical shape after detaching from the injection nozzle.

Deformation of bubble under pressure-driven flow is primarily affected by the pressure difference between gas and melt phases, shear stress, and the melt flow rate. The cone-shaped bubble head and the fishtail-shaped trailing end were both results of the above factors.

Bubble volume also has a significant effect on its deformation. On the one hand, the decreased bubble volume will make the capillary number small, thus the deformation is reduced, and on the other hand, the little gas fractional coverage along height of the flow channel will make the interface deformation caused by the flow field decrease relatively.

In the investigation of the parameters relevant to bubble detachment, the gas injection pressure, the melt pressure near the injection port, and the screw rotation speed were changed separately. The results show that the maximum diameters of the bubbles will experience peak values upon detaching from the injection nozzle, whereas the variation of bubble volume and the surface area are dependent on the pressure difference between the gas injection pressure and the melt pressure. The high pressure difference will make them continue to increase after detaching from the nozzle.

The melt flow rate and the pressure difference both have critical effects on the injected bubbles. Increasing the melt flow rate is favorable to achieve little bubbles in short time, while the result of increasing pressure difference is just the opposite. Therefore, in order to acquire little bubbles in short time during practical gas injection process, the higher melt flow rate and low pressure difference should be maintained.

Relative to the practical production, the experimental result still has its limitations since it is obtained in the experimental apparatus and low gas injection pressure and melt pressure are utilized. Therefore, the experimental result should be scaled up in the larger apparatus so that it can be applied in practice, and more work will be done in the future.

Acknowledgments

This work has been supported by the National Nature Science Foundation under grant No. 10172074/A020205, Guangdong Province Nature Science Foundation under grant No. 04011554, Guangdong Province Science and Technology Program under grant No. 2003C103015.

References

1. L. CHARLES, TUCKER III and PAULA MOLDENAERS, *Annu. Rev. Fluid Mech.* **34** (2002) 177.
2. G. O. SHONAIKE and G. P. SIMON, "Polymer Blends and Alloys" (Marcel Dekker: New York, 1999) p. 1.
3. L. A. UTRACKI and Z. H. SHI, *Polym. Eng. Sci.* **32** (1992) 1824.
4. L. CHEN, X. WANG, R. STRAFF and K. BLIZARD, *ibid.* **42** (2002) 1151
5. S. LEE, T. *ibid.* **33** (1993) 418.
6. J. A. BIESENBERGER and S. T. LEE, *ibid.* **26** (1986) 982.
7. *Idem.*, *ibid.* **27** (1987) 510.
8. *Idem.*, *ibid.* **29** (1989) 782.
9. M. FAVELUKIS, Z. TADMOR and R. SEMIAT, *AIChE. J.* **45** (1999) 691.
10. Y. C. PENG, M. C. GUO, L. LI and K. L. LI, *J. Mater. SCI. Lett.* **22** (2003) 639.
11. Z. L. CHEN, "Doctoral Thesis" (South China University of Technology, 2000) p. 89.
12. C. D. HAN and H. J. YOO, *Polym. Eng. Sci.* **21** (1981) 518.
13. C. D. HAN, "Rheology in Polymer Processing" (Academic Press, New York, 1976) p. 165.

Received 19 October
and accepted 17 December 2004